

# Interactions between CAP70 and actinfilin are important for integrity of actin cytoskeleton structures in neurons

Ying Chen, Min Li \*

*Department of Neuroscience and High Throughput Biology Center, Johns Hopkins University School of Medicine, BRB311, 733 North Broadway, Baltimore, MD 21205, USA*

Received 20 February 2005; received in revised form 11 May 2005; accepted 26 May 2005

## Abstract

The integrity of dynamic actin structures is coupled to a variety of neurological processes. Actin-binding proteins play a critical role in regulating actin structure dynamics. A link between actin-binding proteins and receptor interacting scaffolding proteins may provide a conduit for transmitting signaling events to the cytoskeleton. Actinfilin is a brain-enriched actin-binding protein, though its functions are currently unknown. We report here that actinfilin interacts with the multi-PDZ domain protein CAP70. Recombinant expression of an actin-binding domain of actinfilin progressively causes marked changes of cellular morphology. The effect on cell morphology may be reduced by co-expression with CAP70. Mutation of actinfilin lacking the ability to interact with CAP70 abolished the effect by CAP70. The evidence suggests a role of actinfilin and possible regulation by scaffolding proteins. © 2005 Elsevier Ltd. All rights reserved.

*Keywords:* Protein interaction; PDZ domain; Molecular organization; Actin cytoskeleton; Postsynaptic density

## 1. Introduction

The dynamic regulation of actin structure is known to be involved in a number of biological processes. Neuronal cytoskeleton plays a role in determining static and dynamic morphology both in terms of overall cell shape and subcellular structures. One such structure is the dendritic spine, a protrusion found in more than 90% of glutamatergic synapses. Spines are postsynaptic subcellular domains, rich in actin and critical for synaptic transmission. Changes in spine shape, number, and/or morphology impact cellular learning and memory (Fifkova and Van Harrevel, 1977; Crick, 1982; Chang and Greenough, 1984; Desmond and Levy, 1988; Bailey

and Kandel, 1993; Toni et al., 1999). The stability and dynamics of actin structures in postsynaptic densities may be regulated by diffusible secondary messages and regulatory protein factors (Matus, 1999; Rao and Craig, 2000). Hence, a combination of chemical signaling and mechanical stability may provide the basis for cross-talk between signaling events and subcellular structures.

CFTR associated protein 70 (CAP70) is a scaffolding protein with four PDZ protein interaction domains which are found in a number of tissues including brain (Kocher et al., 1998; Wang et al., 2000). Actinfilin is a novel brain-enriched protein that was cloned on the basis of its interaction with CAP70 (Chen et al., 2002). Actinfilin is homologous to *Drosophila Kelch*, which has a characteristic amino-terminal BTB/POZ domain that is involved in homomeric or heteromeric protein–protein interactions (Li et al., 1992; Aravind and Koonin, 1999). In addition, to the C-terminus there are six homologous kelch domains that are thought to form a beta-propeller

\* Corresponding author. Tel.: +1 410 614 5131; fax: +1 410 614 1001.

*E-mail address:* [minli@jhmi.edu](mailto:minli@jhmi.edu) (M. Li).

structure conferring binding to F-actin (see review by Adams et al., 2000). While much evidence has accumulated from genetic studies with regard to Kelch's role in morphogenesis of the *Drosophila* ovarian ring canal (Robinson et al., 1997), its precise biochemical and cell biological function remains unknown. Recently, another Kelch-related protein has been identified which is associated with giant axonal neuropathy (GAN) (Bomont et al., 2000), hence named gigaxonin. Gigaxonin has an essentially identical domain organization to actinfilin. This further raises questions concerning the biochemical and physiological roles of kelch domain containing proteins.

Actinfilin is found specifically in brain and concentrated in, but not limited to, dendritic terminals including postsynaptic densities that are also concentrated with actin (Matus et al., 1982; Chen et al., 2002). Purified actinfilin interacts with F-actin suggesting that it interacts with actin structures *in vivo*. Because of actinfilin interactions with both actin structures and CAP70, and the likely interaction between CAP70 and receptors and/or channels, it is of importance to investigate actinfilin interactions with CAP70 and their potential effects on cell morphology.

Here we report a series of biochemical and cell biological experiments to investigate the possible roles of actinfilin. The activities of actinfilin in neurons were studied with a truncated form which corresponds to the actin-binding domain. The effects of CAP70 on actinfilin were examined by combinatorial co-expression. Expression of the actin-binding domain of actinfilin disrupted the F-actin structures and led to marked changes of neuronal morphology. The results provide evidence of macromolecular organization including actinfilin, CAP70 and actin.

## 2. Methods

### 2.1. Materials

Molecular cloning reagents were purchased from New England Biolabs (Beverly, MA) or Promega (Madison, WI). Glutathione sepharose-4B was from Amersham Pharmacia (Piscataway, NJ). Fluorescein or Texas red dye conjugated goat anti-rabbit IgG and horse anti-mouse IgG was from Jackson Labs (West Grove, PA, 1:250 for immunocytochemistry). Rabbit anti-PSD95 antibody (1:5000 for immunoblotting and 1:2000 for immunohistochemistry) and rabbit anti-CAP70 antibody (1:2000 for immunoblotting and 1:500 for immunohistochemistry) were generated against glutathione-S-transferase (GST) fusion protein, and rabbit anti-actinfilin antibody (1:5000 for immunoblotting and 1:200 for immunohistochemistry) was generated against maltose binding protein (MBP) fusion protein. Rabbit

anti-synGAP antibody (1:500 for immunoblotting) and mouse anti-PSD95 antibody, clone K28/43 (1:100 for immunohistochemistry) were from Upstate Biotechnology (Lake Placid, NY). Goat anti-rabbit lactose dehydrogenase (LDH) (1:500 for immunoblotting) and mouse anti-NR1 antibodies (1:2500 for immunoblotting and 1:100 for immunohistochemistry) were purchased from Chemicon International (Temecula, LA). Mouse anti-flag (M5, 1:2500 for immunoblotting) and mouse anti-HA antibodies (F-7, 1:2500 for immunoblotting) were from Sigma (St. Louis, MO). Fluorescein or rhodamine-conjugated phalloidin were from Molecular Probes (Eugene, OR) (1:50 for immunocytochemistry). And all other reagents were purchased from Sigma (St. Louis, MO), except as indicated.

### 2.2. Yeast two-hybrid screen

Full length CAP70 was subcloned into yeast expression vector pPC97 in a fusion with the GAL4 DNA binding domain. This construct was transformed in yeast strain PJ69-4a (MATa trp1-90i leu2-3112 ura 3-52 his3-200 gal4Δ gal80Δ GAL2-ADE2 LYS2::GAL1-HIS3 met2::GAL7-lacZ) (James et al., 1996) by the lithium acetate method (Straus and Ausubel, 1990). Transformants were selected on leucine<sup>-</sup> (Leu<sup>-</sup>) medium and subsequently transformed with an oligo-dT-primed rat hippocampal cDNA library subcloned into vector pPC86 (gift of Dr. Paul Worley). Positive clones were selected on the basis of growth in triple-selection media (Leu<sup>-</sup>, Trp<sup>-</sup>, and Adenine<sup>-</sup>). The plasmids were isolated using RPM Yeast Plasmid Isolation Kit (BIO 101, Vista, CA) and transformed into *Escherichia coli* HB101. The *E. coli* clones containing the pPC86 construct were rescued, and the plasmids were isolated. The positive clones were cotransformed into yeast PJ69-4a with either the bait vector or the original pPC97 vector to determine bait-dependent growth.

### 2.3. Immunoblot analysis of developmental expression of CAP70 protein in rat brain

Postnatal days 2–20, day 24 and adult brains of Sprague–Dawley (SD) rats were harvested and ground in liquid nitrogen. The powder (20 mg) was solubilized in 250 μL SDS solubilization buffer (1% w/v 2-(*N*-cyclohexylamino) ethanesulfonic acid (CHES), 2% w/v SDS, 1% w/v DTT, 10% v/v glycerol, pH 9.5). Then an equal amount of SDS sample buffer was added. The samples were boiled for 5 min. Each sample (5 μL (200 μg)) was load onto 10% SDS-PAGE and transferred to NC membranes. Anti-CAP70 antibody was for immunoblot analysis.

#### 2.4. *In situ* hybridization

*In situ* hybridization was performed using a digoxigenin (DIG)-RNA labeling kit (Boehringer Mannheim, Indianapolis, IN). Briefly, DNA templates for RNA probe synthesis were prepared by digesting plasmid containing the full length rat CAP70 cDNA. After linearization, DIG-labeled RNA probes were prepared by *in vitro* transcription. Frozen horizontal sections (12  $\mu\text{m}$ ) of adult male SD rat brain were used to analyze the CAP70 mRNA distribution. All solutions were prepared in deionized  $\text{H}_2\text{O}$  treated with 0.1% (v/v) diethylpyrocarbonate and autoclaved. Prehybridization was carried out at 4 °C overnight with prehybridization solution (50% formamide, 5 $\times$  SSC, 5 $\times$  Denhardt's solution, 250  $\mu\text{g}/\text{mL}$  yeast tRNA, and 500  $\mu\text{g}/\text{mL}$  salmon sperm DNA). For hybridization, the sections were covered with a prehybridization solution containing 1  $\mu\text{g}/\text{mL}$  of cRNA probe and incubated at 65 °C overnight in a humid chamber. Sections were immersed sequentially in 0.2 $\times$  SSC twice and buffer 1 (0.1 M Tris-HCl, pH 7.5, 0.15 M NaCl) twice. The sections were covered by 1:2000 anti-DIG antibody in buffer 2 (1% inactivated normal goat serum in buffer 1) and incubated at 4 °C overnight. After rinsing with buffer 1 and buffer 3 (0.1 M Tris-HCl, pH 9.5, 0.1 M NaCl, and 50 mM  $\text{MgCl}_2$ ), the sections were developed with a solution containing 1.2 mg levamisole and 300  $\mu\text{L}$  NBT/BCIP in 5 mL development buffer containing 0.1 M Tris (pH 9.5), 0.1 M NaCl, and 50 mM  $\text{MgCl}_2$ .

#### 2.5. Immunohistochemistry staining

Immunohistochemical staining of adult male SD rat brain was performed on horizontal 20  $\mu\text{m}$  microtome sections using rabbit or mouse antibodies at the dilutions as described in Section 2.1. The antibody binding was visualized using biotin-conjugated secondary antibody. Vectastain ABC kit (Vector Laboratories, Burlingame, CA) was used to visualize the immunocomplex in the sections.

Cultured neurons grown on poly-L-lysine-coated 18-mm diameter glass coverslips were washed with phosphate-buffered saline (PBS), fixed for 20 min with 4% paraformaldehyde in PBS, and permeabilized for 15 min with 0.2% Triton X-100 in PBS. Then the samples were sequentially exposed to primary and secondary antibodies in immuno-staining buffer (5% normal goat serum, 5% normal horse serum, 5% BSA, and 0.1% Triton X-100 in PBS) for 1 h at room temperature. Primary antibody dilutions are described in Section 2.1. Fluorescent-conjugated secondary antibodies were used at a 1:250 dilution. The mounted coverslips were viewed with an Ultraview confocal microscope.

#### 2.6. Subcellular fractionation

Cell fractionation studies were performed using brain homogenates from adult SD rats as described by Carlin (Carlin et al., 1980). Briefly, ~5 gm of fresh cerebellum was homogenized in 50 mL of 320 mM sucrose buffer (320 mM sucrose, 1 mM  $\text{NaCO}_3$ ) (sample was saved as brain lysate) and centrifuged for 10 min at 1400  $\times g$ . The supernatant was saved, and the pellet was then homogenized again in the same 50 mL buffer and spun for 10 min at 710  $\times g$ . The supernatant was pooled with the supernatant from the previous spin and spun for 10 min at 755  $\times g$  (the supernatant were saved as s2. The pellet was resuspended to 50 mL in the same buffer and saved as p2). The supernatant (s2) was spun again for 10 min at 13,800  $\times g$ . The supernatant was saved as s5. This pellet was resuspended and homogenized in 12 mL low salt buffer (320 mM sucrose, 1 mM  $\text{NaCO}_3$ ) (sample was saved as p5) and loaded onto a sucrose gradient (0.85 M sucrose, 1.0 M sucrose and 1.2 M sucrose in 1 mM  $\text{NaCO}_3$ ). After a 2 h spin at 82,500  $\times g$ , the sample above 0.85 M sucrose, the sample between 0.85 and 1.0 M sucrose, the sample between 1.0 and 1.2 M sucrose and the sample of the pellet were resuspended in 30 mL of low salt buffer, yielding 6g1, 6g2, 6g3 and 6g4 fractions. The 6g3 was named as the synaptosomal fraction in previous literature (Chen et al., 1998). The 6g3 synaptosomal fraction was solubilized by adding 30 mL 1% ice-cold Triton X-100 in low salt buffer for 15 min and centrifuged at 32,000  $\times g$  for 20 min. The pellet was resuspended in 1.25 mL low salt buffer loaded onto a sucrose gradient (1.0 M sucrose, 1.5 M sucrose and 2.0 M sucrose in 1 mM  $\text{NaCO}_3$ ). The Triton 1 PSD fraction was recovered between 1.5 and 2.0 M sucrose after a spin at 201,800  $\times g$  for 2 h. The Triton 1 PSD fraction was resuspended in 6 mL low salt buffer and further solubilized again by adding 6 mL 1% Triton X-100 (1% Triton X-100 in 150 mM KCl). The PSD fraction was centrifuged at 210,800  $\times g$  for 20 min. The pellet was resuspended in 200 mL of 40 mM Tris-HCl (pH 8.0) and saved as Triton 2 PSD fraction. For probing the presence of CAP70 in the PSD, the protein concentration was determined by DC protein assay kit (Bio-Rad Laboratories Inc., Hercules, CA). Saved samples (5  $\mu\text{g}$ ) were separated by 10% SDS-polyacrylamide gel and immunoblotted with antibodies for NR1, GluR2, CAP70, synGAP or LDH (Ye et al., 2000).

#### 2.7. Co-immunoprecipitation

For co-immunoprecipitation in heterologous cells, COS7 cells were transfected with different combinations of constructs. At 48 h post transfection, cells were washed twice with PBS and lysed in 200  $\mu\text{L}$  lysis buffer (10 mM Tris-HCl (pH 8.0), 1% Triton X-100, 15 M NaCl, 1 mM EDTA, 10 mM  $\text{NaN}_3$ , and protease

inhibitor cocktail (1 mM phenylmethylsulfonyl fluoride, 1  $\mu\text{g}/\text{mL}$  leupeptin, 2  $\mu\text{g}/\text{mL}$  aprotinin and 1  $\mu\text{g}/\text{mL}$  pepstatin)) at room temperature for 30 min. The supernatant was collected after centrifugation of the lysates at  $27,000 \times g$  for 1 h at  $4^\circ\text{C}$ . An aliquot of 50  $\mu\text{L}$  of the supernatant was incubated with corresponding antibody and 20  $\mu\text{L}$  of protein A-sepharose (1:1 slurry) in 200  $\mu\text{L}$  of lysis buffer overnight at  $4^\circ\text{C}$ . The mixture was washed three times with PBS (containing 0.5 M NaCl). The proteins were eluted with 30  $\mu\text{L}$  SDS sample buffer. An aliquot of 10  $\mu\text{L}$  from each sample was separated by 10% SDS-polyacrylamide gel. Immunoblot analysis was performed with the indicated antibodies.

Immunoprecipitations from rat brain homogenates were performed according to a published protocol (Dunah et al., 1998). Briefly, a total of 800  $\mu\text{L}$  extract was incubated with antibodies  $4^\circ\text{C}$  overnight. Precipitates were washed with binding buffer twice (50 mM Tris-HCl, pH 8.0, pH 7.4, 0.1% Triton X-100) and resuspended in 70  $\mu\text{L}$  of SDS sample buffer. Then 10  $\mu\text{L}$  of each sample was separated by 10% SDS-polyacrylamide gel. Immunoblot analysis was performed with the indicated antibodies.

### 2.8. Co-sedimentation study

The pGEX4T2 plasmid was modified by adding one Tobacco Etch V N1a protease (TEV) cleavage site flanked by two domains of the Gly-Gly-Gly-Gly-Ser (G4S) sequence between GST and the downstream fusion protein. *E. coli* BL21 cells were used to express the GST-TEV-kelch domain protein, and the recombinant protein then was purified by GST sepharose-4B column. The kelch domain protein was eluted from the column by TEV protease and further purified using Mono-Q ion exchange chromatography. The resulting fractions were analyzed by SDS-PAGE before being pooled together and concentrated. The rabbit skeletal muscle globular actin (G-actin) was purchased from Cytoskeleton (Denver, CO). The ability of the kelch domain of actinfilin proteins to associate with F-actin was examined by co-sedimentation assays with modification (Bailey and Kandel, 1993). The kelch domain proteins were pre-cleaned by centrifugation at  $100,000 \times g$  for 1 h at  $4^\circ\text{C}$ . Kelch domain proteins and G-actin were mixed in 100  $\mu\text{L}$  F-actin polymerization buffer (5 mM imidazole [pH 7.0], 50 mM KCl, 1 mM  $\text{MgCl}_2$ , 0.2 mM ATP, 1 mM EGTA, and 0.5 mM DTT) at room temperature for 2 h. The samples were centrifuged at  $30,000 \times g$  for 20 min at  $4^\circ\text{C}$ . SDS sample buffer (100  $\mu\text{L}$  in  $2 \times$  concentrated stock) was added to the supernatant, and the pellets were resuspended in 100  $\mu\text{L}$  1XSDS sample buffer. An aliquot of 10  $\mu\text{L}$  of supernatant or 5  $\mu\text{L}$  of the pellet from each sample was analyzed by SDS-PAGE and visualized with

Coomassie blue staining. In the co-sedimentation experiment of kelch domain protein with actin, immunoblotting with anti-actinfilin antibody was used to examine the presence and absence of the kelch domain protein in each sample, because of the similar protein molecular weight of kelch domain protein and actin.

### 2.9. Neuronal culture and transfection

Cortical neurons from embryonic day 17 SD rats were cultured according to the procedure of Ghosh and Greenberg (Ghosh et al., 1994), except that the cells were maintained in neurobasal medium supplemented with B27 supplements (Invitrogen, Carlsbad, CA). For transfection studies, low density cortical neurons were transfected at 3–5 days in vitro with different combinations of plasmids. The transfection was carried out by the calcium phosphate method. The neurons were then stained at 2 days after the transfection for young neurons and at about 2 weeks after the transfection for mature neurons.

### 2.10. Quantification of the changes of cell morphology

For HeLa cells, the cells were transfected at 50% confluence with mixed Eugene 6 (Roche, Indianapolis, IN) and different plasmid combinations for 4 h, then the medium was changed and cells were allowed to grow for the indicated time periods. For confocal imaging, the cells were fixed and stained with rhodamine-phalloidin on the second day after transfection. For morphology quantification, the live cells were imaged directly by ZEISS fluorescent microscopy with a  $10 \times$  lens. The rounded-up cells were determined using two following criteria: (1) whether the cell was very well extended in both GFP fluorescence and differential interference contrast (DIC) images; (2) the volume of the cells on the DIC image.

For neurons, the transfection was carried out by the calcium phosphate method. For confocal imaging, neurons were fixed and stained with rhodamine-phalloidin on the third day after transfection. The phalloidin binds to F-actin at the junction between subunits (Steinmetz et al., 1998) and has similar affinity for both large and small filaments. It has been used as a way to monitor the depolymerization of the filamentous actin (Shorte, 1997).

## 3. Results

### 3.1. Neuronal expression of CAP70

A CAP70 antibody identified a single CAP70 band in most tissues but detected two very closely migrating bands of 70 kDa in brain. The specificity of antibody

binding is characterized by peptide competition (Wang et al., 2000). During development, expression of the CAP70 upper band could be detected as early as day 4, becoming obvious on day 10. The expression of the CAP70 lower band was not detectable until day 10 and reached a similar level to that of the upper band on day 24. Both bands were found in maximal level in the adult rat brain (Fig. 1A). The location of CAP70 in different rat brain regions was analyzed at the mRNA level by *in situ* hybridization (Fig. 1B) and at the protein level by immunohistochemistry (Fig. 1D). Strong hybridization signals were found in hippocampal and cerebellar regions of the adult rat brain (Fig. 1B). In contrast, the sense probe showed no detectable hybridization (data not shown). Anti-CAP70 antibodies were used to detect protein localization in different regions of rat brain using successive sections. CAP70 was localized in various regions of brain including cortex, hippocampus, and cerebellum. The most prominent staining was in the pyramidal cells in cingulate cortex layer 5 of cerebral cortex and CA1 region of hippocampus. In cerebellum, both Purkinje cells and granule cells were positive. The staining of all three regions was concentrated mostly in the soma and the dendritic processes (Fig. 1D, the right panels). Using specific antibodies for actinfilin and PSD95, we have previously shown considerable overlap in their protein localization (Chen et al., 2002). To more accurately compare the protein distribution with that of actinfilin, we visualize these proteins using the serial adjacent sections (Fig. 1D). Overall, the distribution of CAP70 has a considerable overlap with that of PSD95 and actinfilin (Kistner et al., 1993; Chen et al., 2002).

To further determine the subcellular localization of the CAP70 protein, isolated cortical neurons in cultures were stained with an affinity purified anti-CAP70 antibody and analyzed by confocal microscopy. The CAP70 signal was found to be diffused throughout the cell and also in small fluorescent puncta along the neurites. Double staining of anti-CAP70 antibodies with antibodies for either PSD95 or NMDA receptor subunit 1 (NR1) displayed different degrees of overlaps with PSD95 and NR1 in the punctated structure (Fig. 1C). This supports a notion of structure heterogeneity within dendritic processes.

Different from what has been found in kidney, CAP70 in brain is insoluble. Even under strong detergent conditions, only a small fraction of CAP70 could be solubilized (data not shown). Immuno-staining of the CAP70 protein both in tissue and in transfected culture showed that the CAP70 was colocalized to the actin-rich subcellular domains in non-neuronal cells (data not shown). The partial colocalization of CAP70 with NR1 and PSD95 at the punctated structures in neurites is consistent with the notion that CAP70 is a component of the postsynaptic density protein complex. To test this hypothesis, postsynaptic density preparations were

obtained using standard techniques (see Section 2), and the resultant protein samples from different steps of the isolation were collected and analyzed by immunoblotting using specific antibodies for CAP70, NR1, GluR2, synGAP and lactose dehydrogenase (LDH). NR1, GluR2, and synGAP were enriched in synaptosomes and resistant to detergent treatments (Fig. 2A, Triton 1 and Triton 2), consistent with previous results (Cho et al., 1992; Kim et al., 1996; Kim et al., 1998). A typical soluble protein, LDH, did not show any enrichment in the insoluble preparations nor did it display any resistance to detergent treatments (Fig. 2A, bottom panel, lanes 5 and 6). The level of enrichment of CAP70 in the synaptosome fraction was not as pronounced as that of other PSD proteins such as synGAP (Fig. 2A, lanes 1 and 4). Instead, CAP70 appeared to be highly enriched in the Triton 1 fraction (Fig. 2A, lane 5). Hence, the evidence is consistent with the notion that CAP70 is a component of postsynaptic densities. This data also suggest that CAP70 may be present in non-PSD microdomains.

### 3.2. Interactions of CAP70 with actinfilin

CAP70 consists of four tandem PDZ domains (Kocher et al., 1998; Wang et al., 2000). This allows it to interact with several other proteins in the brain by nucleating protein complexes. To search for possible CAP70-associated proteins, a yeast two-hybrid screen was performed using CAP70 full length cDNA as bait. Plasmids of positive clones were rescued and confirmed by retransformation and growth selection. Multiple independent clones of candidate interacting proteins have been identified (see Section 2). These include synaptic RasGAP (synGAP) and SAP90/PSD95-associated proteins (SAPAP), both of which are present in the nervous system and found in the PSD protein complex. In addition, we also found at least two additional novel genes, designated as clones 6 and 14. The coding sequences of these two clones differ in the C-terminal domains but have a similar amino-terminal POZ/BTB domain (pox virus and zinc finger) or T1 domain in potassium channels. The BTB/POZ or T1 domains are involved protein–protein interactions and ion channel subunit assembly (Li et al., 1992; Ahmad et al., 1998; Kreusch et al., 1998; Wong and Privalsky, 1998). Clone 6 is the rat isoform of the SETA binding protein 1 (SB1) gene (Borinstein et al., 2000). The homomeric interactions of clone 6 and clone 14 were detected, suggesting a role in oligomerization *in vivo*.

Clone 14 is actinfilin that we reported earlier (Chen et al., 2002). To further analyze interactions between CAP70 and actinfilin, we constructed flag-tagged full length actinfilin. The immunoprecipitation experiments were performed with protein A agarose conjugated with either anti-flag antibody for actinfilin or anti-HA

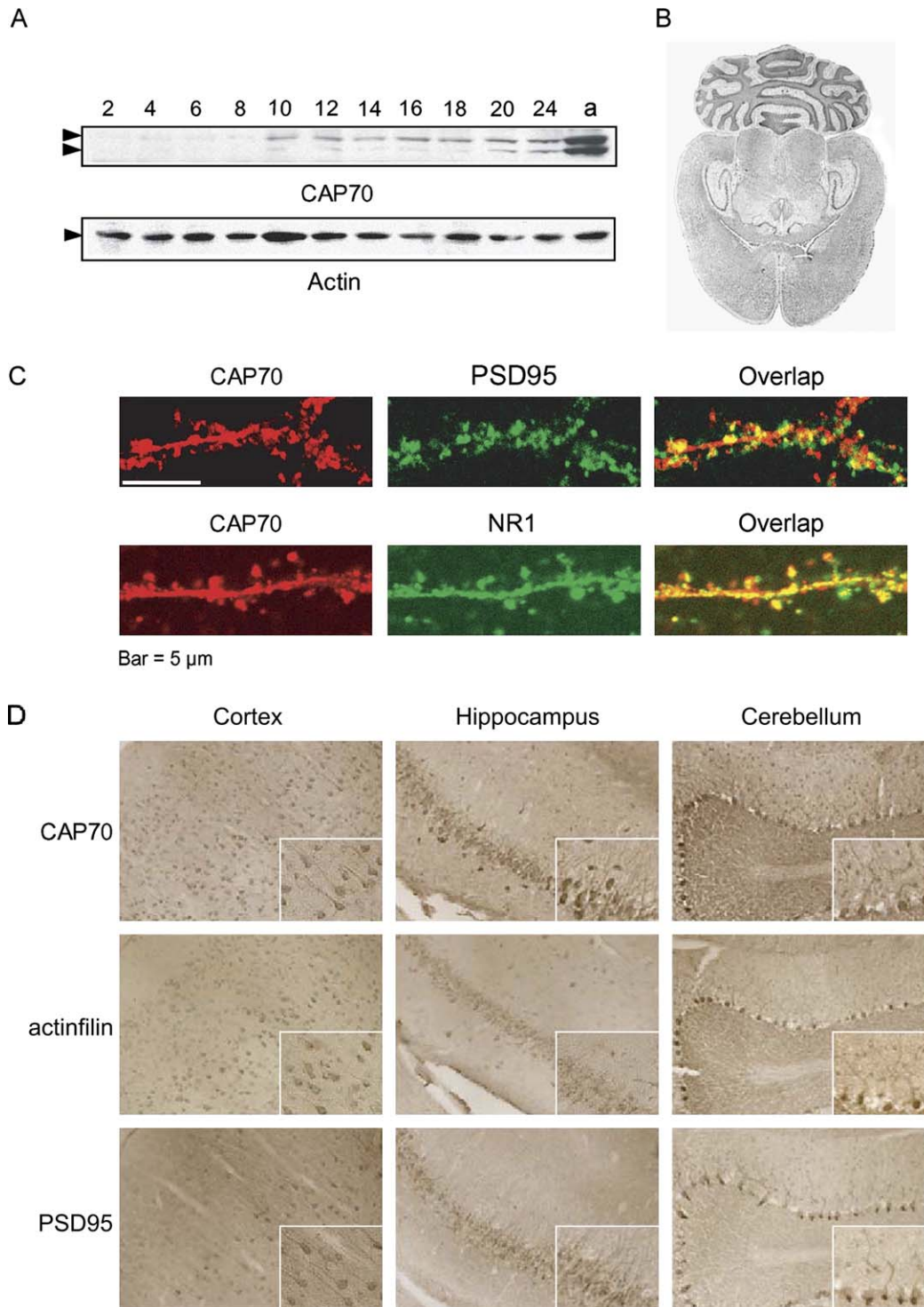


Fig. 1. Developmental expression, brain distribution and subcellular localization of CAP70 protein. (A) Expression of CAP70 during postnatal development of the rat brain. Rat brain tissue lysates were prepared from the rats for every other day from day 2 to day 20, day 24 and adult. A total of 200  $\mu$ g of tissue lysate from each sample was analyzed by immunoblotting. The postnatal day of the samples is indicated on the top of the gel. The two CAP70 bands are indicated on the left. The same amount of tissue lysate was analyzed by immunoblotting with anti-actin antibody to calibrate protein loading in all lanes. (B) In situ hybridization detection of mRNA encoding CAP70 in rat brain. Horizontal sections of adult rat brain were hybridized with DIG-labeled antisense probe (Section 2), which was generated using full length of mouse CAP70 cDNA. (C) Colocalization of CAP70 and postsynaptic protein in cultured cortical neurons. Low density mature cortical neurons, 21 days in vitro culture (DIV21), were stained with antibodies against proteins as indicated on the top of each image and imaged with a confocal microscope. Top panels – double labeling of the cortical neurons for endogenous CAP70 and PSD95, with the merged color image as indicated. Bottom panels – double labeling of the cortical neurons for endogenous CAP70 and the NR1 subunit of the NMDA receptor with the merged color image as indicated. (D) Immunohistochemistry detection of the CAP70 protein in rat brain. Consecutive sections of rat brain were stained with the antibodies against actinfilin, PSD95 and CAP70 as indicated on the left of the panel (Section 2). The regions of sections, cerebral cortex, hippocampus, and cerebellum, are indicated on the top. The sections were viewed with a bright field light microscope with 20 $\times$  objective lens. Higher magnification views are shown in the inserts.

antibody for CAP70. Following immunoprecipitation, immunoblotting with either anti-HA antibodies or anti-flag antibodies was carried out to detect precipitated polypeptides. CAP70 and actinfilin were co-immunoprecipitated either by anti-flag antibody or by anti-HA antibody (Fig. 2B, lanes 4 and 8). In contrast, the actinfilin lacking the last three amino acids did not show co-immunoprecipitation with CAP70 (Fig. 2B, lanes 3 and 7). This result is in good agreement with a direct interaction between PDZ domain-mediated CAP70 and the C-terminus of actinfilin.

To determine whether CAP70 and its associated proteins form a protein complex in brain tissue, the interactions of CAP70, actinfilin, and synGAP in solubilized brain extracts were tested by performing co-immunoprecipitation (Fig. 2C). Antibodies for CAP70 and PSD95, but not HA were able to co-immunoprecipitate other PSD proteins including synGAP, actinfilin and the NR1 subunit of the NMDA receptor (Fig. 2C, lanes 2, 5 and 6). The anti-actinfilin antibody was able to co-immunoprecipitate PSD95, synGAP but was not able to effectively co-immunoprecipitate NR1 (Fig. 2C, lane 3), and the anti-synGAP antibody was able to co-immunoprecipitate PSD95, NR1 and actinfilin (Fig. 2C, lane 4). While, anti-CAP70 precipitated synGAP and actinfilin, the signal of CAP70 immunoprecipitated by anti-actinfilin and anti-synGAP was not detectable. This may be caused by the very limited solubility of CAP70 (Fig. 2A). The precipitates were also immunoblotted by anti-GluR2 antibody. No signal was found in any of the immunoprecipitates, although GluR2 could be detected in the input sample (Fig. 2C, lane 1), supporting the specificity of antibodies used in immunoprecipitation. This provides evidence that the NR1 subunit of the NMDA receptor, PSD95, synGAP and CAP70 are in the same or overlapping protein complexes. Although both CAP70 and actinfilin have very limited solubility, the ability of anti-CAP70 antibody to precipitate actinfilin (Fig. 2C, lane 2) is indicative that actinfilin is connected to the protein complex. This is consistent with the role of CAP70 in organization of the protein complex including actinfilin, synGAP, and NMDA receptors.

Previous work showed that different PDZ domains of CAP70 possess different binding affinities for the CFTR carboxyl terminus. Multivalent binding is important for CAP70 to regulate CFTR channel activity (Wang et al., 2000). To characterize the association of CAP70 with its binding proteins, constructs for HA and GFP double tagged individual PDZ domains of CAP70 were made (Fig. 3A). Our yeast two-hybrid screen for CAP70 binding proteins has identified actinfilin, SB1 and synGAP. Co-immunoprecipitation experiments were carried out to test the binding preference of flag-tagged actinfilin, SB1 and synGAP to individual PDZ domains of CAP70. PDZ domains 1, 3 and 4 were capable of

interacting with actinfilin (Fig. 3C, upper panels). Precipitation of the PDZ1 domain was more efficient than that of PDZ3 or PDZ4, consistent with the notion that the PDZ1 domain has the highest affinity. The interaction of SB1 with various PDZ domains displayed a similar specificity profile (Fig. 3C, middle panels). In contrast, PDZ3 appeared to have the highest affinity interaction with synGAP compared to other PDZ domains (Fig. 3C, lower panels). The binding preference of synGAP is similar to that of CFTR (Wang et al., 2000). This interaction preference may stem from their C-terminal interaction motifs: TSL (actinfilin), TSF (SB1), TRV (synGAP) and TRL (CFTR) (Fig. 2B). The –1 position, Ser for actinfilin and SB1 but Arg for synGAP and CFTR, may be responsible for the differential binding preference. The localization of CAP70 and actinfilin in cultured neurons has significant overlaps (data not shown), in agreement with the notion of CAP70–actinfilin interaction *in vivo*.

### 3.3. Actinfilin interactions with F-actin

Actinfilin is a brain-enriched protein found in the postsynaptic densities and in the shaft of dendrites (Chen et al., 2002). Purified glutathione-S-transferase (GST)-kelch fusion protein was sufficient to interact with F-actin in the presence or absence of phalloidin (data not shown). Because actinfilin has a BTB/POZ domain that mediates homomeric interactions, it is believed that native actinfilin oligomerizes and is therefore capable of bundling F-actin filaments. Our previous experiments were performed with GST fusion of kelch domain (Chen et al., 2002), to directly demonstrate that the interaction is indeed mediated by the kelch domain and that the monomeric kelch domain is sufficient for binding, a tobacco etch virus (TEV) protease site was engineered between GST and kelch (see Section 2). The resultant kelch domain (a.a. 287–639) protein was cleaved off, purified, and confirmed by mass spectrometry (Fig. 4A). An increasing concentration of F-actin induced dose-dependent kelch precipitation with F-actin (Fig. 4B, lanes 4, 6, and 8). The interaction between actinfilin and F-actin was also visualized by electron microscopy after negatively staining the purified proteins. The purified kelch domain alone was found to decorate F-actin filaments. GST-kelch was able to bind and bundle F-actin filaments presumably via a weak GST–GST interaction (data not shown). To image F-actin and actinfilin in native cells, the cortical neuronal cultures (20 days *in vitro* culture) were stained with anti-actinfilin antibody and rhodamine-conjugated phalloidin to visualize F-actin. Actinfilin showed small fluorescent puncta staining distributed along the neurites and the soma. In the neurites, the punctated staining of actinfilin was partially overlapped with F-actin structure (Fig. 4C).



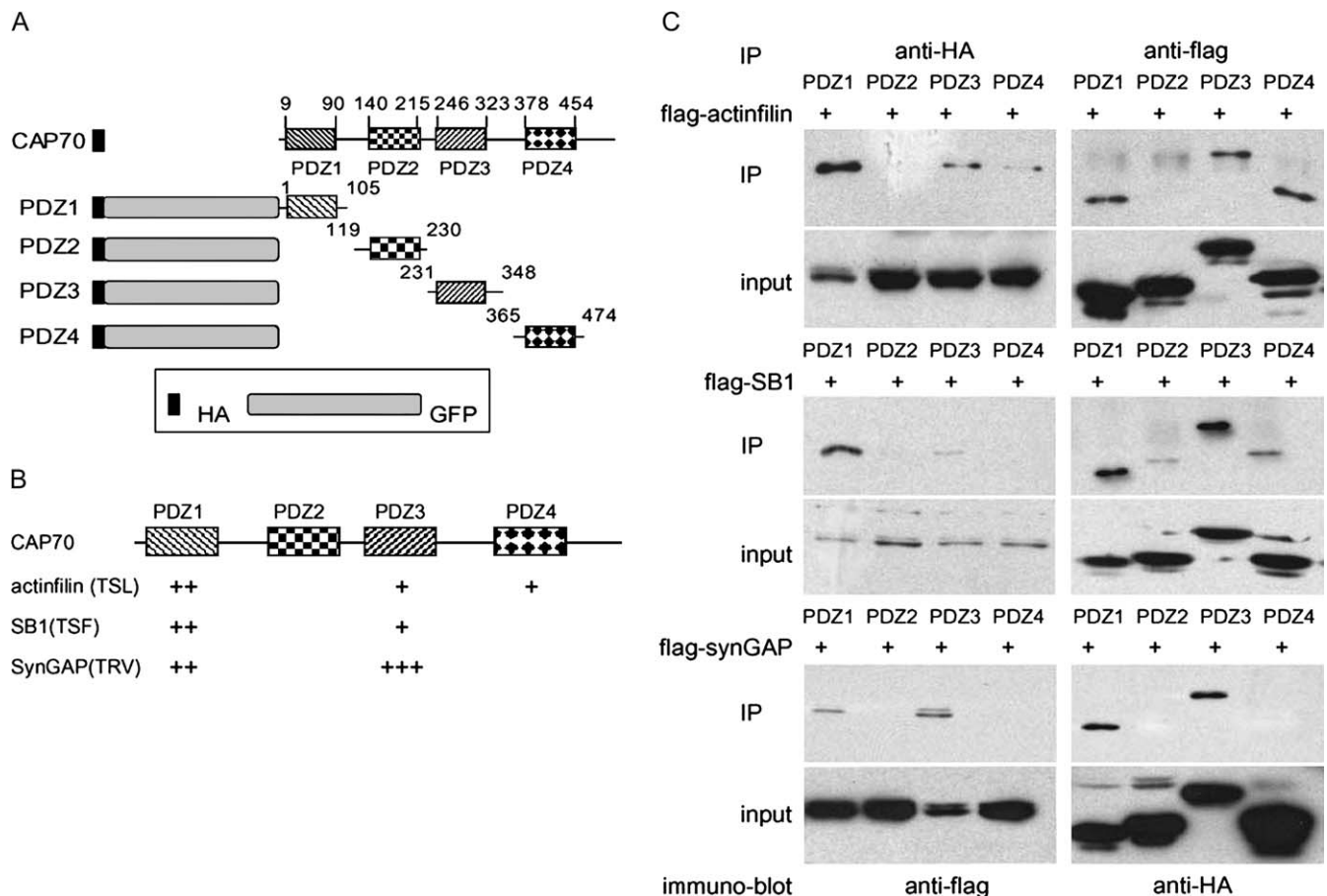


Fig. 3. Differential interactions between individual PDZ domains of CAP70 and its associated proteins. (A) Schematic diagrams of HA- and GFP-fusions of the full length or the individual PDZ domains of CAP70. The amino acid positions corresponding to the CAP70 amino acid sequences are indicated. (B) A schematic diagram summarizing the binding preference derived from immunoprecipitation experiments. (C) Actinfilin, SB1 and synGAP associate with different PDZ domains of CAP70 in transfected COS7 cells. COS7 cells were transfected using different combinations of plasmids as indicated on the top of each gel. Presence of CAP70 and its individual PDZ domains are indicated by their name, and presence or absence of SB1, actinfilin and synGAP are marked as “+”. The soluble cell lysates were immunoprecipitated with anti-flag or anti-HA antibodies, and the immunoprecipitants were separated by 10% SDS-PAGE. After transfer to nitrocellulose membrane, the immunoprecipitated polypeptides were detected by antibodies indicated at the bottom of the gels.

studied. The transient expression of the GFP-kelch fusion resulted in morphological changes of HeLa cells, characteristically rounding up. Such changes in morphology coincide with the loss of stress fiber staining in HeLa cells (Fig. 5A). The extent of morphological changes was time-dependent, where the expression of the kelch domain gave rise to a more pronounced effect at 72 h after transfection than that at 24 h (Fig. 5B, right panels). The majority of the kelch domain-expressing cells eventually dislodged from the culture dishes. In contrast, the expression of a GFP construct did not cause any noticeable change in either cell number or morphology.

The protein expression and the corresponding morphological changes have been quantified (Fig. 6A and B). In cells that have been transfected with either GFP or GFP-kelch, the total numbers of GFP positive cells have been determined at 24, 48 and 72 h after transfection. Of the GFP positive cells, those with the “rounded-up”

morphology have been quantified. The ratios of “rounded” cells vs. GFP positive cells (“transfected”) are shown in histograms (Fig. 6B). At 72 h after transfection, more than 85% GFP-kelch transfected cells exhibited substantial morphological changes resulting in loss of attachment. In contrast, less than 20% GFP transfected cells displayed changes of morphology (Fig. 6B). The differential effects by GFP and GFP-kelch were not due to the lack of expression, as the protein levels of GFP were detectable at 24 h after transfection and present in comparable amounts at 48 and 72 h after transfection (Fig. 6A). This result is indicative that the kelch domain, presumably via its ability of binding to actin, is causal in changing HeLa cell morphology.

### 3.5. Rescuing activity of CAP70–actinfilin interactions

The differential interactions of four PDZ domains of CAP70 with CFTR channel potentiate CFTR channel

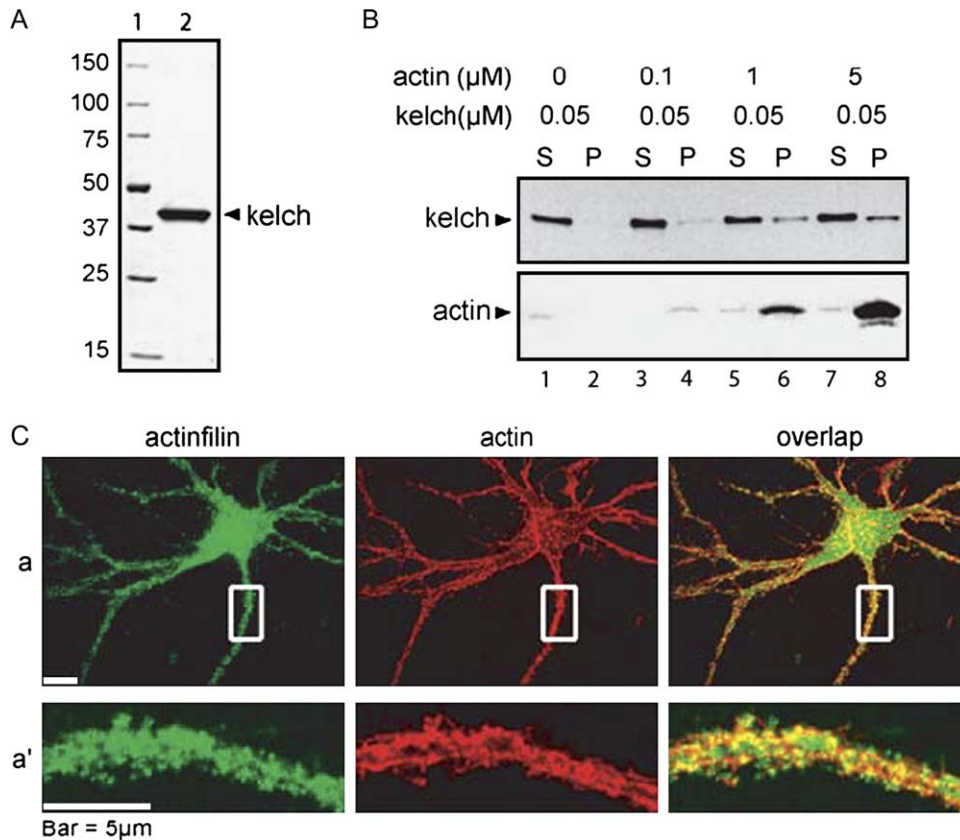


Fig. 4. Association of actinfilin protein with filamentous actin. (A and B) Association of the kelch domain of actinfilin protein with filamentous actin in vitro. The kelch domain protein (kelch) of actinfilin was purified as described in Section 2. (A) Purified kelch domain protein (0.5  $\mu\text{g}$ ) was assayed by SDS-PAGE. (B) The association of kelch domain protein with filamentous actin was tested by co-sedimentation assay. The final concentration of actin and kelch domain protein is indicated on the top of the gel. The band corresponding to actin or kelch domain protein is indicated on the left. The actin is shown by coomassie blue stained SDS-PAGE (lower panel), and the kelch domain protein is shown by immunoblotting with anti-actinfilin antibody (upper panel). The supernatant (S) and the pellet (P) were loaded in the same amounts on the gel and are indicated above the gel. (C). Colocalization of actinfilin with F-actin in cultured cortical neuron. Low density mature cortical neurons (21 days in vitro) were stained with anti-actinfilin antibody and rhodamine-conjugated phalloidin to visualize F-actin and imaged with a confocal microscope. (a) Punctate staining of endogenous actinfilin is colocalized with actin structure in cultured cortical neuron. Double labeling of the endogenous actinfilin protein, actin structure, and the overlapped image as indicated. The boxed regions are shown in higher magnification in the corresponding lower panels.

activity (Wang et al., 2000). In brain tissue and cultured neurons, CAP70 protein has considerable overlap with that of actinfilin (Fig. 1D, and data not shown). It is curious whether the CAP70–actinfilin interactions have any effect on morphological changes. To test this, HA-CAP70 was co-expressed with the GFP-kelch domain, and the morphological changes of GFP positive cells were monitored and quantified using the procedure described above (Fig. 6C, Section 2). Co-transfection of CAP70 with GFP-kelch reduced the “rounded-up” cell ratio from  $86.4 \pm 2.4\%$  to  $47.0 \pm 1.6\%$  (Fig. 6C, #2 & #4). This effect is not related to possible reduction of kelch expression as a result of competing expression of another protein because co-transfection of an unrelated HA-fusion protein (G3BP) did not alter the effectiveness of the kelch domain in mediating morphological changes (Fig. 6C, #6). Co-expression of other interacting proteins such as PSD95 instead of CAP70 displayed no rescuing effect (data not shown).

The suppression (rescue) of kelch-induced morphological changes by CAP70 may originate from several possible mechanisms. For example, CAP70 may confer biochemical activities downstream, hence suppressing the effects of the kelch domain. Another possibility is CAP70 interacts with the kelch via PDZ domain interactions (Fig. 3). To test the role of PDZ domain-mediated interaction, the effect of CAP70 was examined using mutants of kelch domain proteins. A deletion mutant of the kelch domain lacking the TSL binding motif was equally effective in causing the cell “rounded-up” morphology at a ratio of  $92.8 \pm 5.0\%$ , but it displayed no sensitivity to the rescuing effect by CAP70 (Fig. 6C, #3 & #5). A substitution of TSL with FCF, which interacts with the PDZ1 domain of *inactivation no afterpotential D* (INAD) (van Huizen et al., 1998), was also no longer sensitive to CAP70 (data not shown). Thus, the direct interaction of CAP70 with the C-terminus of the kelch domain is likely to be responsible for the rescue effects.

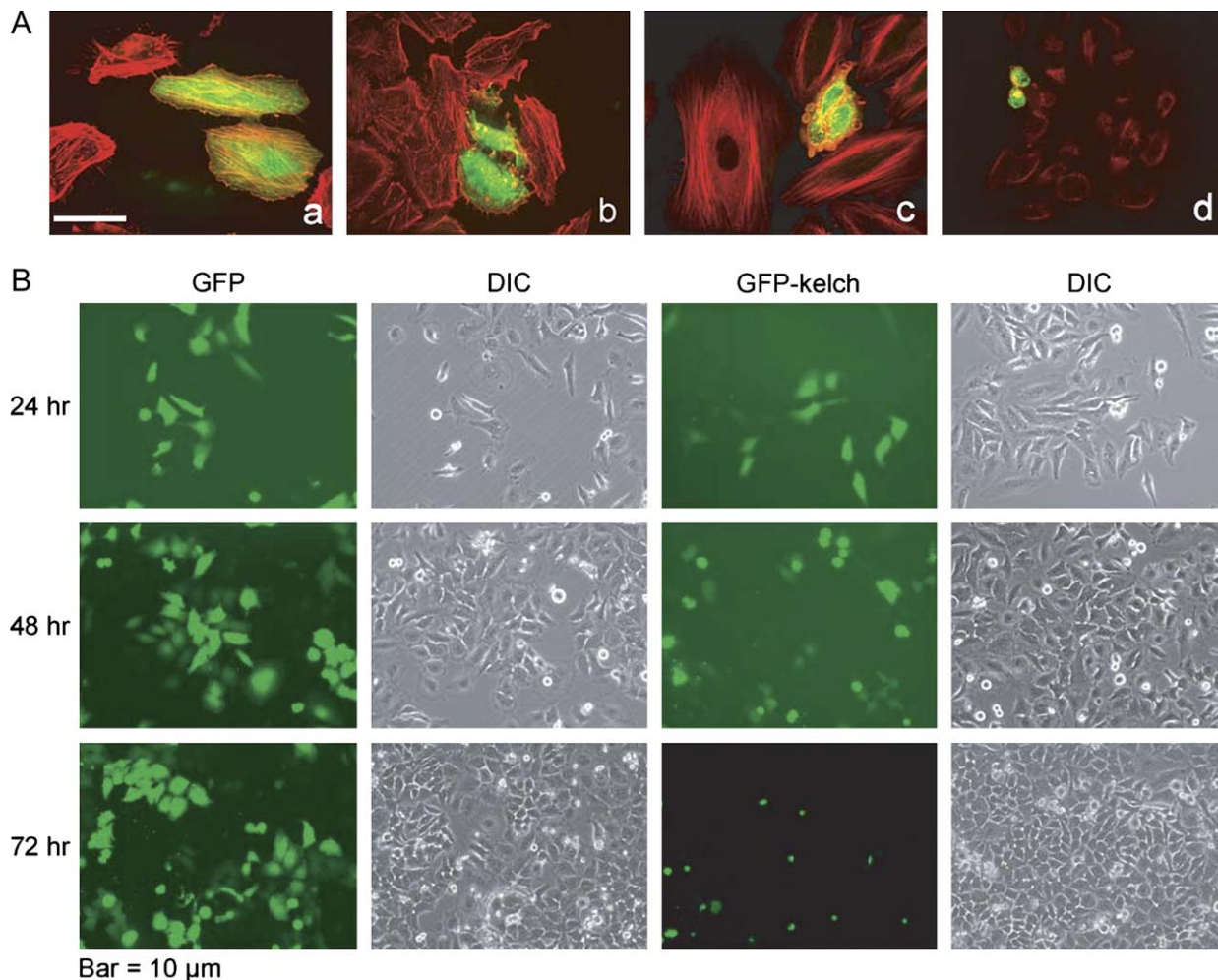


Fig. 5. Induction of the “rounded-up” morphology change in HeLa cells by over-expression of the kelch domain of actinfilin protein. (A) Diverse morphology of HeLa cells 24 h after transfection with the GFP-kelch domain of actinfilin construct. The GFP fluorescent signal is evenly distributed inside the cell, and the cell has very typical actin stress fibers (a). GFP signal is aggregated in the cell, and no stress fiber is in the transfected cells (b). Both GFP and actin stainings show the fragmentation of the cytoplasm (c). Cells are rounded-up, with the majority of cells losing attachment to the bottom of the culture plate (d). (B) HeLa cells were transfected with the GFP-kelch domain construct. The integrity of the actin structure was imaged by a confocal microscope after labeling cells with rhodamine-phalloidin at 24 h after transfection. The overall morphology changes in the HeLa cells after transfection were tracked by GFP fluorescent and DIC images at 24, 48 and 72 h. Tracking of the morphology changes after the transfection at 24, 48 and 72 h as indicated on the left side of the images. The cells were either transfected with GFP construct or the GFP-kelch domain construct as indicated on the top.

To monitor the effect of kelch domain in neurons, primary cortical neurons were transfected, and the morphological changes were tracked by staining neurons with rhodamine-phalloidin at different times after transfection. At 48 h post transfection, major morphological changes could be observed in the transfected neurons. The actin and kelch protein could be seen in the soma and the neurites. Phalloidin-binding signal and GFP with fused kelch domain were very well colocalized in a small percentage of transfected, surviving neurons (Fig. 7A, b & b1). While in most of the transfected neurons the actin organization was disrupted (Fig. 7A, c & d, and e & f). In contrast, GFP transfected neurons displayed normal actin organization (Fig. 7A, a). Because the phalloidin has no effect in biochemical binding assay between kelch and F-actin (Chen and Li, unpublished results), the disap-

pearance of phalloidin signal is consistent with reduction of F-actin structure accessible to phalloidin binding. The kelch expression in the transfected neurons and the actin cytoskeleton changes were quantified. The ratios of the transfected neurons displayed no phalloidin-binding signal versus the total number of transfected neurons (GFP positive) are shown in the histogram (Fig. 7C). At 48 h after transfection, about  $90 \pm 2\%$  of neurons transfected with the kelch construct showed disintegration of actin cytoskeleton (Fig. 7B). In contrast, approximately  $20 \pm 4\%$  of neurons transfected with the GFP construct showed some degree of disruption in the actin structures. This is similar to the findings in HeLa cells (Fig. 6). In the kelch and CAP70 cotransfected neurons, the ratio was reduced to about  $67 \pm 3\%$ . Detection of surviving neurons after the kelch transfection

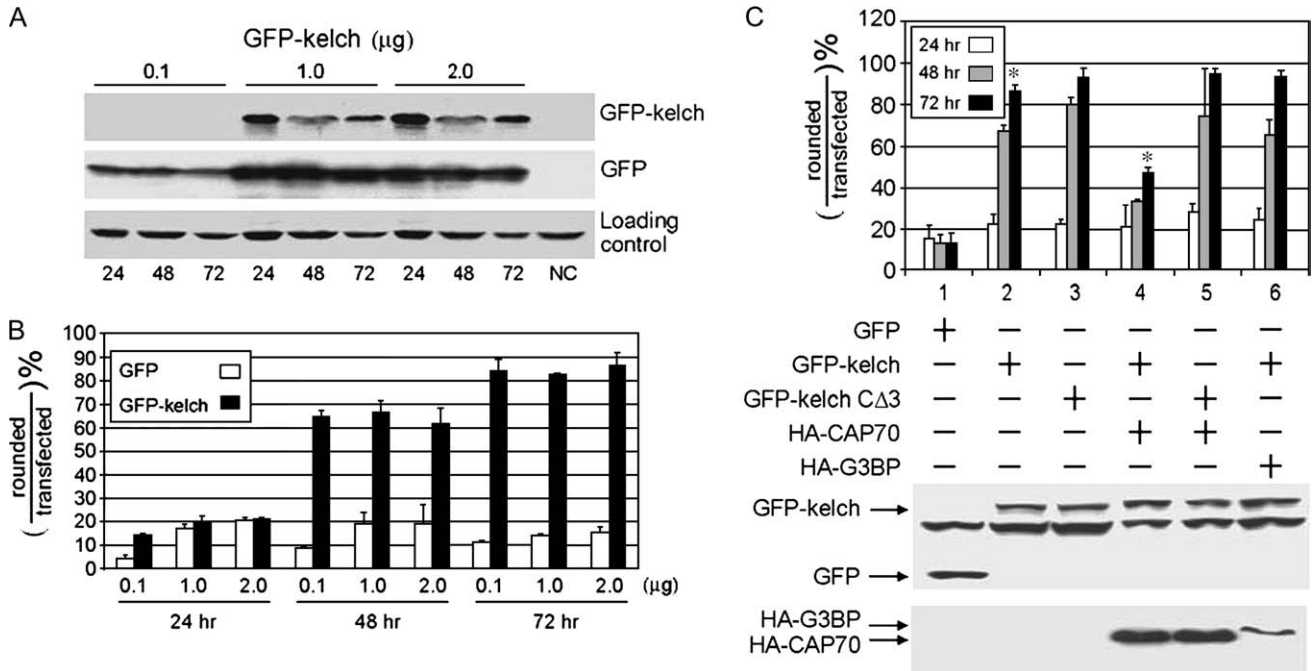


Fig. 6. Quantification of the morphology changes in HeLa cells. (A) Expression of GFP and GFP-kelch domains of the actinfilin construct. The protein expression level of the corresponding constructs was determined by immunoblotting with an anti-GFP antibody. Lysate for 10,000 cells of each sample was separated by SDS-PAGE and transferred to a nitrocellulose filter, then analyzed by immunoblotting. The transfected cells were harvested at the time point as indicated at the bottom of the gel. The amount of plasmid used in the transfection is indicated on the top of the gel, the GFP-kelch domain protein and the GFP protein are indicated to the right. The loading control is displayed at the bottom panel. (B) A histogram of the percentage of rounded cells GFP-kelch transfected cells. Different amounts of DNA used in the transfection are indicated at the bottom of the histogram, as are the time points when the expression and morphology changes were monitored. The details are described in Section 2. The ratios of the number of “rounded-up” GFP fluorescence positive cells vs. the total number of GFP fluorescence positive cells are plotted as a percentage. For each sample, a minimum of 200 GFP fluorescence positive cells were counted and two independent experiments were carried out for each sample. (C). Suppression of the effects of the kelch domain by co-expression with CAP70 in HeLa cells. Upper panel. A histogram displays the ratios of rounded cell vs. total transfected cells at indicated time points. The different combinations of transfection are shown below. The protein expression in each combination is monitored at 24 h by immunoblot using either anti-GFP (upper panel) or anti-HA (lower panel). The corresponding bands of the GFP-kelch/kelchΔ3 domain of actinfilin, GFP, HA-CAP70 and HA-G3BP proteins are indicated to the left of the gels.

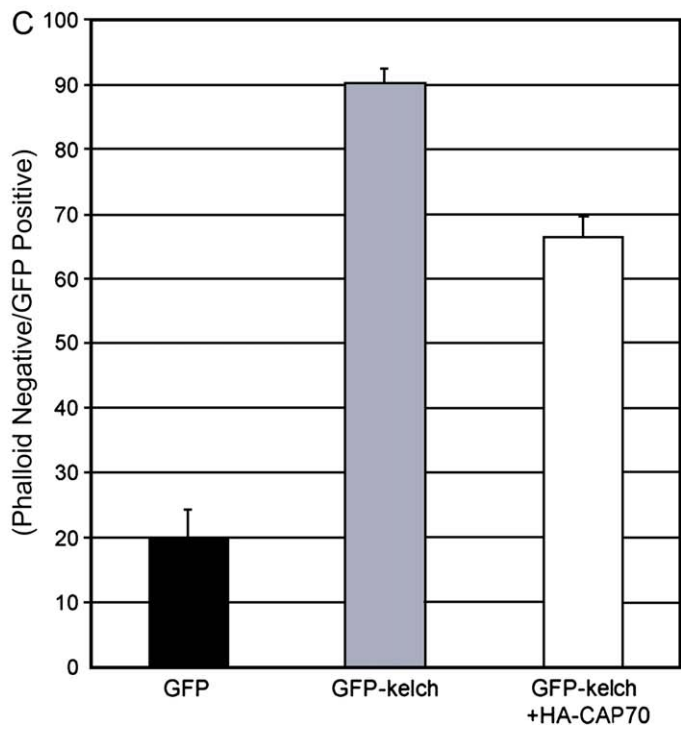
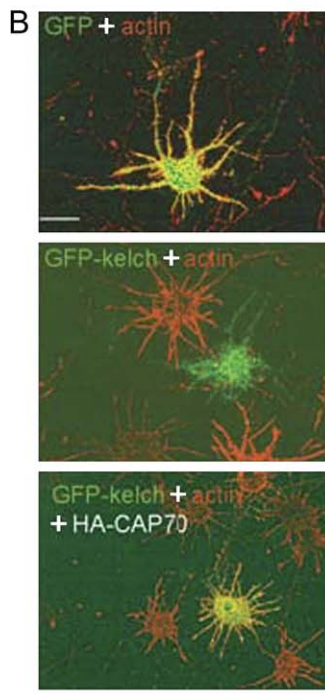
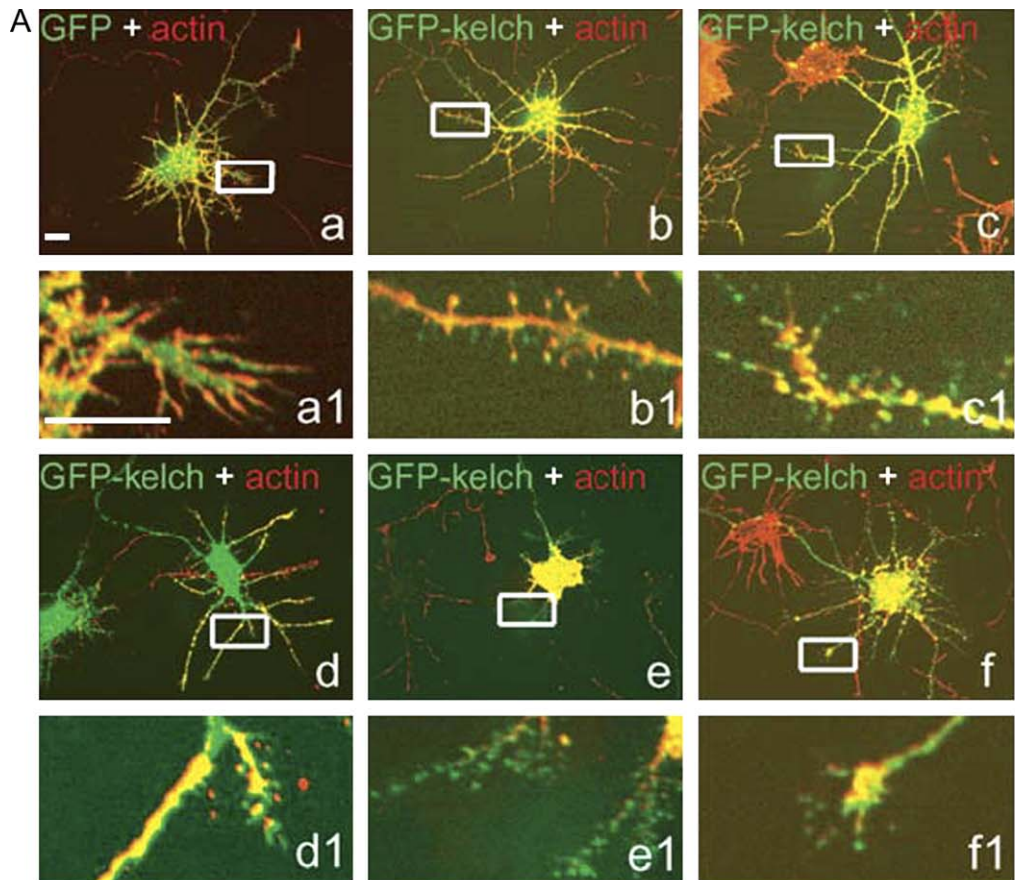
was not successful in mature neurons. In contrast, when co-expressing CAP70, mature neurons expressing the kelch domain were readily observed (data not shown), indicating that the CAP70 effect was stable in non-dividing neurons. These results suggest that the changes of actin cytoskeleton organization in the neurons were caused by recombinant expression of the kelch domain of actinfilin protein, and this effect can be suppressed by co-expression of the CAP70 protein.

**4. Discussion**

The kelch domain has been found in a variety of proteins. Their functional roles are diverse, including enzymatic catalysis, transcription, recombination, and interaction with cytoskeleton structures (see review by Adams et al., 2000). The interaction of the kelch domain with F-actin has been recognized from both genetic studies in which *Kelch* confers proper morphology of actin-rich intracellular canals (Xue and Cooley, 1993)

and biochemical studies that demonstrate the interaction with F-actin in vitro (Robinson et al., 1997; Kim et al., 1999; Adams et al., 2000; Chen et al., 2002). The precise role of interactions with F-actin has not been fully established. This is in part due to the lack of an assay to monitor its activity in culture. The perturbation of F-actin in cultured cells reported here has opened the opportunities to investigate its role in detail within a specific cell biological context.

The ability to interact with F-actin indicates that actinfilin is a member of actin-binding proteins. Several classes of actin-binding proteins have been identified, including actin-depolymerizing factors (ADF)/cofilins, profilins, gelsolins, thymosin, DNase I, capping proteins, and actin related protein (Arp) 2/3 complexes (see review by dos Remedios et al., 2003). These proteins confer a variety of activities ranging from globular (G)-actin sequestering to polymerization inhibition via catalysis (e.g., ADF/cofilin), end capping (e.g., tropomodulin), or serving (e.g., gelsolin). Other classes of actin-binding proteins appear to play a role in organizing large



structures by cross-linking of filamentous (F)-actin (e.g., actin related protein (Arp) 2/3) or stabilizing actin filaments to prevent depolymerization (e.g., tropomyosin). Hence, these activities confer both diversity and plasticity of actin structures, giving rise to the rich biology of actin structures in eukaryotes (see reviews by Bamberg, 1999; Higgs and Pollard, 2001). Actinfilin and *Drosophila Kelch* are similar in a number of ways, including similar domain organizations and interactions with F-actin. Unique to actinfilin is the striking tissue specific expression in neurons (see Fig. 1 and Chen et al., 2002). The high degree of conservation both in terms of amino acid sequence and in terms of biochemical binding to F-actin presents a special challenge to dissecting the functional roles of actinfilin and the related proteins. The questions may be addressed at two different resolutions. The first approach would be to genetically remove the gene (such as actinfilin) or to reduce the expression level via techniques such as RNA interference (RNAi). Information resulting from these kinds of studies would provide insights into what aspects of physiological processes actinfilin may affect. The second approach would be to focus the question(s) on the functional role concerning one specific aspect of activity, i.e. the actinfilin–CAP70 interaction and actinfilin–F-actin interaction. The RNAi approach was effective to reduce recombinant actinfilin expression but showed no effect on native actinfilin expression, presumably due to the long half life of actinfilin protein (data not shown). The present report attempts to address this question by studying interactions in vitro and in cultured cells. The purified recombinant kelch domain of actinfilin, either in monomeric form or in dimeric form (GST fusion), is sufficient to bind to F-actin. The binding may be detected by co-sedimentation assays (Chen et al., 2002) and imaged by electron microscopy. The evidence reported in this paper shows that kelch binding to F-actin is an important interaction critical for the integrity of actin structures. The over-expression of kelch, presumably via binding to F-actin, hence disrupting a native interaction, induced dramatic morphological changes. Despite the tissue specific expression of actinfilin in brain, the physiological role conferred by actinfilin kelch is conserved in other cells, such as HeLa cells (Figs. 5 and 7). It is not known but certainly of great interest to test whether actin-binding kelch domains found in other

kelch domain containing proteins may also cause the morphological changes of the actin cytoskeleton. It is important to point out that the experimental evidence present here does not rule out possible additional activity for kelch domain or for actinfilin. Mel-26 is a member of BTB domain containing proteins. Different from actinfilin, Mel-26 has a MATH domain at the C-terminus, which plays a role in recruiting substrate for ubiquitination pathway (Pintard et al., 2003).

The interaction of CAP70 with actinfilin abolishes the effects of the kelch domain (Figs. 6 and 7). The effects were observed in both transiently transfected dividing HeLa cells and non-dividing cultured neurons. CAP70 may exert such an effect by two different mechanisms. One would be that the CAP70 interaction results in a loss of actinfilin interaction with F-actin. Such inhibition may be either competitive or non-competitive with regard to the modes by which actinfilin interacts with F-actin and CAP70. Our evidence from in vitro binding experiments suggests that the binding of kelch to F-actin is not affected by purified CAP70 (data not shown). This argues against the notion that the effect found in the cultured cells was due to the loss of actinfilin binding to F-actin by CAP70. Hence, one likely possibility is that the CAP70-mediated rescuing effect is caused by a combination of CAP70 binding with specific sub-cellular localization of CAP70. This is an interesting topic of future investigation. CAP70 was isolated on the basis of its binding to cystic fibrosis transmembrane conductance regulator (CFTR). It potentiates CFTR channel activities by multivalent interactions which recruit two CFTR molecules into a transition dimer (Wang et al., 2000). This appears to be an important mechanism for regulating CFTR channels (Kleizen et al., 2000; Bezprozvanny and Maximov, 2001). There are several lines of evidence suggesting that CAP70 may have multiple interaction partners. First, it is expressed abundantly in a number of tissues including kidney, liver, small intestine, and brain. Some of these tissues express little or no CFTR. Second, within a given tissue such as kidney where the CAP70 is found, the protein level is considerably more abundant than that of CFTR. Third, recent evidence also has indicated CAP70 interaction with scavenger receptor B, type I (SR-BI), which regulates the level of receptor surface expression (Silver, 2002; Madjdpour et al., 2004). Thus, CAP70 may

Fig. 7. (A). Effects of the kelch domain of actinfilin protein in neurons. A GFP-kelch construct was transfected into cultured cortical neurons on day 5. Neurons were fixed, and the actin structures were labeled by rhodamine-phalloidin 48 h after transfection. Neurons were then imaged by a confocal microscope. The neuron was transfected by GFP construct and showed GFP in green and actin in red (a). The boxed growth cone region was showed in high magnification in (a1). The neurons were transfected by the GFP-kelch domain construct and showed GFP signal in green and actin in red (b, c, d, e and f). The boxed regions are shown correspondingly in high magnification (b1, c1, d1, e1 and f1). (B). Reduction of the effects of the kelch domain by CAP70 in neurons. Images of neurons transfected with indicated constructs are shown. (C) The effect by kelch was quantified as described in Section 2. Two independent transfections and at least 100 neurons were scored for each sample. The percentage of the phalloidin-negative neurons of the transfected (GFP positive) neurons is plotted as a histogram in the right panel. The combinations of the constructs used in the transfection are indicated at the bottom of the histogram. An example image for each sample is shown on the left panel, and the transfection and staining are as indicated.

participate in different biological processes and investigation of CAP70 interaction partners may provide additional insights into its functional roles. The ability of CAP70 to bind several neuronal proteins, such as synGAP, SB1 and SAPAP, suggests possible roles of CAP70 in organizing protein complexes. Interestingly, interactions with individual PDZ domains display different binding preferences (Fig. 3). The differential binding preference of PDZ domain containing scaffolding proteins has been seen in a number of cases including PSD95 (Cho et al., 1992), glutamate receptor interacting protein (GRIP) (Dong et al., 1997) and INAD (van Huizen et al., 1998; Xu et al., 1998). Distinct binding specificity of tandem PDZ domains in these proteins provides an attractive mechanism by which one scaffold could recruit multiple interaction partners in order to achieve both specificity and stoichiometry. Thus, CAP70 may function by linking actin structures to receptor/channel signal effectors.

The critical role of kelch binding to the actin structure also raises an interesting question concerning the disease mechanism caused by a similar protein known as gigaxonin, which was first identified from patients who suffer giant axonal neuropathy (GAN) (Bomont et al., 2000; Bruno et al., 2004). This protein possesses a domain organization essentially identical to that of actinfilin. Distinct from actinfilin is its ability to interact with microtubule components (Ding et al., 2002). Intriguingly, several mutations found in human patients are localized within the POZ/BTB domain, presumably resulting in loss of oligomerization (Bomont et al., 2003). This raises the question of whether the mutated protein functions similarly to the kelch domain, which displays a potent effect in our experiments. It would be of interest to examine the potential functional parallel of actinfilin and gigaxonin.

## Acknowledgments

We thank Dr. Jianping Gong for performing the *in situ* hybridization, Dr. Shusheng Wang for various CAP70 constructs, Rachel Derin and Matt Spieker for technical assistance, and Dr. Douglas Robinson for advice. We also thank Drs. Craig Montell, Alex Kolodkin, Douglas Robinson and members of Li lab for valuable comments on this manuscript. The work is supported by grants from the National Institutes of Health (to M.L.) and an Established Investigator Award from the American Heart Association.

## References

- Adams, J., Kelso, R., Cooley, L., 2000. The kelch repeat superfamily of proteins: propellers of cell function. *Trends Cell Biol.* 10, 17–24.
- Ahmad, K.F., Engel, C.K., Prive, G.G., 1998. Crystal structure of the BTB domain from PLZF. *Proc. Natl Acad. Sci. U.S.A.* 95, 12123–12128.
- Aravind, L., Koonin, E.V., 1999. Fold prediction and evolutionary analysis of the POZ domain: structural and evolutionary relationship with the potassium channel tetramerization domain. *J. Mol. Biol.* 285, 1353–1361.
- Bailey, C.H., Kandel, E.R., 1993. Structural changes accompanying memory storage. *Annu. Rev. Physiol.* 55, 397–426.
- Bamburg, J.R., 1999. Proteins of the ADF/cofilin family: essential regulators of actin dynamics. *Annu. Rev. Cell Dev. Biol.* 15, 185–230.
- Bezprozvanny, I., Maximov, A., 2001. PDZ domains: more than just a glue. *Proc. Natl Acad. Sci. U.S.A.* 98, 787–789.
- Bomont, P., Ioos, C., Yalcinkaya, C., Korinthenberg, R., Vallat, J.M., Assami, S., Munnich, A., Chabrol, B., Kurlemann, G., Tazir, M., Koenig, M., 2003. Identification of seven novel mutations in the GAN gene. *Hum. Mutat.* 21, 446.
- Bomont, P., Cavalier, L., Blondeau, F., Ben Hamida, C., Belal, S., Tazir, M., Demir, E., Topaloglu, H., Korinthenberg, R., Tuysuz, B., Landrieu, P., Hentati, F., Koenig, M., 2000. The gene encoding gigaxonin, a new member of the cytoskeletal BTB/kelch repeat family, is mutated in giant axonal neuropathy. *Nat. Genet.* 26, 370–374.
- Borinstein, S.C., Hyatt, M.A., Sykes, V.W., Straub, R.E., Lipkowitz, S., Boulter, J., Bogler, O., 2000. SETA is a multifunctional adapter protein with three SH3 domains that binds Grb2, Cbl, and the novel SB1 proteins. *Cell. Signal.* 12, 769–779.
- Bruno, C., Bertini, E., Federico, A., Tonoli, E., Lispi, M.L., Cassandrini, D., Pedemonte, M., Santorelli, F.M., Filocamo, M., Dotti, M.T., Schenone, A., Malandrini, A., Minetti, C., 2004. Clinical and molecular findings in patients with giant axonal neuropathy (GAN). *Neurology* 62, 13–16.
- Carlin, R.K., Grab, D.J., Cohen, R.S., Siekevitz, P., 1980. Isolation and characterization of postsynaptic densities from various brain regions: enrichment of different types of postsynaptic densities. *J. Cell Biol.* 86, 831–845.
- Chang, F.L., Greenough, W.T., 1984. Transient and enduring morphological correlates of synaptic activity and efficacy change in the rat hippocampal slice. *Brain Res.* 309, 35–46.
- Chen, H.J., Rojas-Soto, M., Oguni, A., Kennedy, M.B., 1998. A synaptic Ras-GTPase activating protein (p135 SynGAP) inhibited by CaM kinase II. *Neuron* 20, 895–904.
- Chen, Y., Derin, R., Petralia, R.S., Li, M., 2002. Actinfilin, a brain-specific actin-binding protein in postsynaptic density. *J. Biol. Chem.* 277, 30495–30501.
- Cho, K.O., Hunt, C.A., Kennedy, M.B., 1992. The rat brain postsynaptic density fraction contains a homolog of the *Drosophila* discs-large tumor suppressor protein. *Neuron* 9, 929–942.
- Crick, F., 1982. Do dendritic spines twitch? *Trends Neurosci.* 5, 44–46.
- Desmond, N.L., Levy, W.B., 1988. Synaptic interface surface area increases with long-term potentiation in the hippocampal dentate gyrus. *Brain Res.* 453, 308–314.
- Ding, J., Liu, J.J., Kowal, A.S., Nardine, T., Bhattacharya, P., Lee, A., Yang, Y., 2002. Microtubule-associated protein 1B: a neuronal binding partner for gigaxonin. *J. Cell Biol.* 158, 427–433.
- Dong, H., O'Brien, R.J., Fung, E.T., Lanahan, A.A., Worley, P.F., Huganir, R.L., 1997. GRIP: a synaptic PDZ domain-containing protein that interacts with AMPA receptors (see comments). *Nature* 386, 279–284.
- dos Remedios, C.G., Chhabra, D., Kekic, M., Dedova, I.V., Tsubakihara, M., Berry, D.A., Nosworthy, N.J., 2003. Actin binding proteins: regulation of cytoskeletal microfilaments. *Physiol. Rev.* 83, 433–473.
- Dunah, A.W., Luo, J., Wang, Y.H., Yasuda, R.P., Wolfe, B.B., 1998. Subunit composition of *N*-methyl-D-aspartate receptors in the

- central nervous system that contain the NR2D subunit. *Mol. Pharmacol.* 53, 429–437.
- Fifkova, E., Van Harrevelde, A., 1977. Long-lasting morphological changes in dendritic spines of dentate granular cells following stimulation of the entorhinal area. *J. Neurocytol.* 6, 211–230.
- Ghosh, A., Carnahan, J., Greenberg, M.E., 1994. Requirement for BDNF in activity-dependent survival of cortical neurons. *Science* 263, 1618–1623.
- Higgs, H.N., Pollard, T.D., 2001. Regulation of actin filament network formation through ARP2/3 complex: activation by a diverse array of proteins. *Annu. Rev. Biochem.* 70, 649–676.
- van Huizen, R., Miller, K., Chen, D.M., Li, Y., Lai, Z.C., Raab, R.W., Stark, W.S., Shortridge, R.D., Li, M., 1998. Two distantly positioned PDZ domains mediate multivalent INAD-phospholipase C interactions essential for G protein-coupled signaling. *EMBO J.* 17, 2285–2297.
- James, P., Halladay, J., Craig, E.A., 1996. Genomic libraries and a host strain designed for highly efficient two-hybrid selection in yeast. *Genetics* 144, 1425–1436.
- Kim, E., Cho, K.O., Rothschild, A., Sheng, M., 1996. Heteromultimerization and NMDA receptor-clustering activity of Chap-syn-110, a member of the PSD-95 family of proteins. *Neuron* 17, 103–113.
- Kim, I.F., Mohammadi, E., Huang, R.C., 1999. Isolation and characterization of IPP, a novel human gene encoding an actin-binding, kelch-like protein. *Gene* 228, 73–83.
- Kim, J.H., Liao, D., Lau, L.F., Haganir, R.L., 1998. SynGAP: a synaptic RasGAP that associates with the PSD-95/SAP90 protein family. *Neuron* 20, 683–691.
- Kistner, U., Wenzel, B.M., Veh, R.W., Cases-Langhoff, C., Garner, A.M., Appeltauer, U., Voss, B., Gundelfinger, E.D., Garner, C.C., 1993. SAP90, a rat presynaptic protein related to the product of the *Drosophila* tumor suppressor gene *dlg-A*. *J. Biol. Chem.* 268, 4580–4583.
- Kleizen, B., Braakman, I., de Jonge, H.R., 2000. Regulated trafficking of the CFTR chloride channel. *Eur. J. Cell Biol.* 79, 544–556.
- Kocher, O., Comella, N., Tognazzi, K., Brown, L.F., 1998. Identification and partial characterization of PDZK1: a novel protein containing PDZ interaction domains. *Lab. Invest.* 78, 117–125.
- Kreusch, A., Pfaffinger, P.J., Stevens, C.F., Choe, S., 1998. Crystal structure of the tetramerization domain of the Shaker potassium channel. *Nature* 392, 945–948.
- Li, M., Jan, Y.N., Jan, L.Y., 1992. Specification of subunit assembly by the hydrophilic amino-terminal domain of the Shaker potassium channel. *Science* 257, 1225–1230.
- Madjdpour, C., Bacic, D., Kaissling, B., Murer, H., Biber, J., 2004. Segment-specific expression of sodium–phosphate cotransporters NaPi-IIa and -IIc and interacting proteins in mouse renal proximal tubules. *Pflugers Arch.*
- Matus, A., 1999. Postsynaptic actin and neuronal plasticity. *Curr. Opin. Neurobiol.* 9, 561–565.
- Matus, A., Ackermann, M., Pehling, G., Byers, H.R., Fujiwara, K., 1982. High actin concentrations in brain dendritic spines and postsynaptic densities. *Proc. Natl Acad. Sci. U.S.A.* 79, 7590–7594.
- Pintard, L., Willis, J.H., Willems, A., Johnson, J.L., Srayko, M., Kurz, T., Glaser, S., Mains, P.E., Tyers, M., Bowerman, B., Peter, M., 2003. The BTB protein MEL-26 is a substrate-specific adaptor of the CUL-3 ubiquitin-ligase. *Nature* 425, 311–316.
- Rao, A., Craig, A.M., 2000. Signaling between the actin cytoskeleton and the postsynaptic density of dendritic spines. *Hippocampus* 10, 527–541.
- Robinson, D.N., Smith-Leiker, T.A., Sokol, N.S., Hudson, A.M., Cooley, L., 1997. Formation of the *Drosophila* ovarian ring canal inner rim depends on cheerio. *Genetics* 145, 1063–1072.
- Shorte, S.L., 1997. *N*-methyl-D-aspartate evokes rapid net depolymerization of filamentous actin in cultured rat cerebellar granule cells. *J. Neurophysiol.* 78, 1135–1143.
- Silver, D.L., 2002. A carboxyl-terminal PDZ-interacting domain of scavenger receptor B, type I is essential for cell surface expression in liver. *J. Biol. Chem.* 277, 34042–34047.
- Steinmetz, M.O., Stoffler, D., Muller, S.A., Jahn, W., Wolpensinger, B., Goldie, K.N., Engel, A., Faulstich, H., Aebi, U., 1998. Evaluating atomic models of F-actin with an undecagold-tagged phalloidin derivative. *J. Mol. Biol.* 276, 1–6.
- Straus, D., Ausubel, F.M., 1990. Genomic subtraction for cloning DNA corresponding to deletion mutations. *Proc. Natl Acad. Sci. U.S.A.* 87, 1889–1893.
- Toni, N., Buchs, P.A., Nikonenko, I., Bron, C.R., Muller, D., 1999. LTP promotes formation of multiple spine synapses between a single axon terminal and a dendrite. *Nature* 402, 421–425.
- Wang, S., Yue, H., Derin, R.B., Guggino, W.B., Li, M., 2000. Accessory protein facilitated CFTR–CFTR interaction, a molecular mechanism to potentiate the chloride channel activity. *Cell* 103, 169–179.
- Wong, C.W., Privalsky, M.L., 1998. Components of the SMRT corepressor complex exhibit distinctive interactions with the POZ domain oncoproteins PLZF, PLZF-RARalpha, and BCL-6. *J. Biol. Chem.* 273, 27695–27702.
- Xu, X.Z., Choudhury, A., Li, X., Montell, C., 1998. Coordination of an array of signaling proteins through homo- and heteromeric interactions between PDZ domains and target proteins. *J. Cell Biol.* 142, 545–555.
- Xue, F., Cooley, L., 1993. Kelch encodes a component of intercellular bridges in *Drosophila* egg chambers. *Cell* 72, 681–693.
- Ye, B., Ye, B., Liao, D., Zhang, X., Zhang, P., Dong, H., Haganir, R.L., 2000. GRASP-1: a neuronal RasGEF associated with the AMPA receptor/GRIP complex. *Neuron* 26, 603–617.